Clathrate Phase in Syndiotactic Polystyrene Gels

Christophe Daniel and Gaetano Guerra*

Dipartimento di Chimica, Università di Salerno, Via S. Allende, 84081 Baronissi (SA), Italy

Pellegrino Musto

Istituto di Ricerca e Tecnologia delle Materie Plastiche del CNR, Via Toiano, 6, 80072 Arco Felice (NA), Italy

Received August 28, 2001; Revised Manuscript Received November 29, 2001

ABSTRACT: Gels and semicrystalline clathrate samples formed by syndiotactic polystyrene (sPS) with 1,2-dichloroethane (DCE) and 1-chloropropane (CP) have been investigated, for the entire composition range from pure solvent to pure polymer, by wide-angle X-ray diffraction (WAXD) and Fourier transform infrared spectroscopy (FTIR). WAXD measurements show that, at least for gels with polymer concentration higher than 0.1 g/g, peaks typical of sPS/DCE and sPS/CP clathrate structures are present. FTIR measurements show the occurrence of the same kind of conformational selectivity for DCE (in favor of the trans conformer) and the absence of conformational selectivity for CP for both gel and clathrate samples. Moreover, the molar ratio between styrenic units and DCE in the crystalline phase of the gels, as evaluated from FTIR data, is nearly constant (3.6 ± 0.3) for the entire composition range; that is close to the 4/1 styrenic unit/guest molecule ratio, which has been observed for the clathrate crystal structure. The whole set of results indicates that the polymer-rich phase forming the cross-link domains of these sPS gels is a crystalline clathrate phase. Both WAXD and FTIR measurements indicate that this clathrate crystalline phase, when present in the gels, would be characterized by coherent lengths being much higher along the chain axes than perpendicular to them.

Introduction

Since its synthesis was first reported in 1986,[1] many studies have focused on the complex polymorphic behavior of syndiotactic polystyrene (sPS).[2−12] In the crystalline state, polymer chains can assume two different skeletal conformations; one is the all-trans planar zigzag structure, and the other is the s(2/1)2 helical conformation (T_2G_2). The chains adopt the trans conformation in the so-called α- and β-crystalline forms while the helical conformation is present in the γ- and δ-forms. In addition to these four crystalline forms, semicrystalline clathrate structures characterized by the helical chain conformation can be obtained by sorption of suitable compounds (mainly halogenated or aromatic hydrocarbons) in amorphous sPS samples as well as in sPS samples being in the α-, γ-, or δ-form. For clathrate structures, both intensities and locations of the reflections in the X-ray diffraction patterns were reported to change only slightly with the kind and the amount of guest molecules.[5,6,9−12] Complete removal of the guest molecules included in clathrate structures can be achieved through suitable solvent treatments, and the δ-form is obtained.[13] The crystal structure of the δ-form, which is characterized by the presence of empty cavities previously occupied by guest molecules in the clathrate forms, has been recently determined.[11] It has been shown that the cavities of the δ-form allow the selective sorption of guest molecules even when present at very low activities.[13a,14]

Recent sorption studies have shown that the conformational equilibrium of guest molecules can be substantially altered as a consequence of clathration into the nanoporous δ-form.[15,16] When 1,2-dichloroethane (DCE) and 1,2-dichloropropane (DCP) are absorbed in the clathrate phase, the trans conformer is largely prevailing while in the amorphous phase the trans and the gauche conformations are nearly equally populated.[15a,c] Conversely, no change of conformational equilibrium was observed for 1-chloropropane (CP).[15c] The high trans selectivity observed for DCE and DCP was explained by electrostatic attractive interactions.[16] Furthermore, by considering the different conformational equilibrium in the amorphous and the clathrate phase, it was possible to evaluate the amount of DCE and diffusion kinetics in both phases.[15b]

Like isotactic polystyrene (iPS) and atactic polystyrene (aPS), sPS is able to form thermoreversible gels in many solvents, and a large body of work has been devoted to sPS gelation. The first reports published by Kobayashi and co-workers dealt with the molecular structure of sPS gels and the kinetics of the gel formation. Fourier transform infrared spectroscopy (FTIR) investigations showed that the gelation process is accompanied by the formation of highly ordered T_2G_2 sequences[5] which could be induced by the clustering of several chain segments but also by the self-organization of a single chain segment into T_2G_2 sequences.[17] Furthermore, it was shown by means of time-resolved small-angle neutron scattering (SANS) experiments that the gel-network structure formation proceeds in parallel to the conformational ordering of sPS chains.[18]

Since then, other reports focusing on the morphology, the thermal behavior, the crystalline structure, and the polymer chain trajectory of sPS gels have been also published. Depending on solvent-type and/or thermal history, two kinds of gel have been reported in the literature: elastic gels characterized by s(2/1)2 helical chain conformation and past-like opaque gels characterized by planar zigzag chain conformation. Gels characterized by helical chains can be transparent in good solvents for polystyrene such as benzene, toluene, or chloroform[5,17−21] or opaque in poorer solvents[19,22−25] such as decahydronaphthalene or *o*-xylene. In big size solvent molecules such as chlorotetradecane or octadecyl

10.1021/ma011531q CCC: $22.00
Published on Web 02/13/2002

benzoate[26] only gels with trans-planar conformation were observed. It is worth noticing that in poor solvents the formation of both kinds of gel can be observed, depending on polymer concentration and/or thermal history.[22−25]

Differential scanning calorimetry (DSC) studies of helical gels have suggested that gelation is accompanied by formation of polymer−solvent compounds whose stoichiometry can differ with the type of solvent.[19,20] However, the thus evaluated stoichiometries of the polymer-rich phase forming the cross-link domains of these gels were found to be quite different from the typical 4/1 monomeric unit/guest molecule stoichiometry determined, for clathrate crystalline structures, by X-ray diffraction studies on fiber clathrate samples.[9,12,27] However, some wide-angle neutron diffraction patterns were found to be qualitatively consistent with X-ray patterns obtained with clathrate samples.[20,21] Hence, the structure of the polymer-rich phase of sPS gels has not been clarified yet, and its stoichiometry remains an open question.[21,28,29]

In this paper we report on FTIR and X-ray diffraction investigations relative to semicrystalline clathrates and gels formed in DCE and CP for the entire composition range from pure solvent to pure polymer. The choice of these two solvents was motivated by the possible additional information which could come from their conformational equilibrium. In fact, a conformational characterization of the solvent molecules should allow to evaluate the amount of DCE confined as a guest into a possible clathrate phase. The purpose of our work is, on one hand, to gain a better understanding of sPS gel structure and, on the other, to investigate possible relationships between sPS gels and clathrates.

Experimental Part

Materials and Sample Preparation. The syndiotactic polystyrene used in this study was manufactured by Dow Chemicals under the trademark Questra 101. ^{13}C nuclear magnetic resonance characterization showed that the content of syndiotactic triads was over 98%. Mass average molar mass obtained by gel permeation chromotography (GPC) in trichlorobenzene at 135 °C was found to be $M_w = 3.2 \times 10^5$ g mol^{-1} with a polydispersity index $M_w/M_n = 3.9$. 1,2-Dichloroethane and 1-chloropropane were purchased from Aldrich and used without further purification.

All sPS gel samples were prepared in hermetically sealed test tubes by heating the mixtures above the boiling point of the solvent until complete dissolution of the polymer and the appearance of a transparent and homogeneous solution had occurred. Then the hot solution was cooled to room temperature where gelation occurred. In DCE it was possible to prepare gel samples up to a concentration of ca. 0.35 g/g while in CP complete dissolution of sPS could be achieved only up to a concentration of 0.15 g/g.

When hot solutions of sPS in DCE are quenched to room temperature, only gels with helical chains are formed while in CP both types of gels can be obtained, depending on the polymer concentration. In particular, when hot solutions are quenched to room temperature, for concentrations below 0.10 g/g, only gels with polymer in the helix conformation are formed, while for concentrations above 0.10 g/g both s(2/1)2 helical and trans-planar sPS conformations can be observed.

Clathrate samples were obtained by immersion of amorphous films in pure solvents at room temperature.

Techniques. X-ray diffraction patterns were obtained on powder samples with nickel-filtered Cu Kα radiation with an automatic Philips diffractometer (PW1710). Gel samples were prepared beforehand in a test tube and reduced in fine powder before data collection was performed while desiccated gel samples were prepared by solvent evaporation in air.

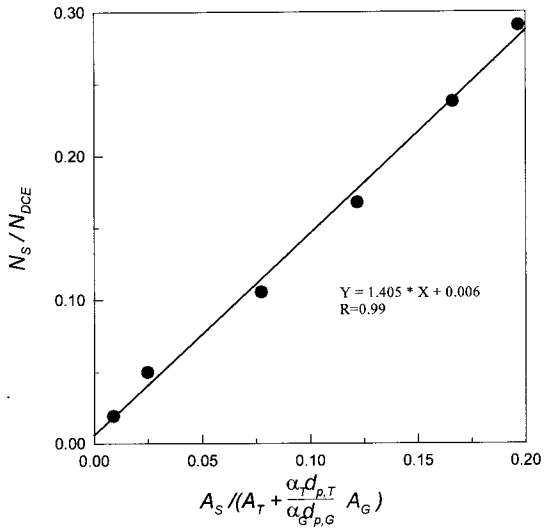

Figure 1. Calibration curve for sPS/DCE gels and ZnSe ATR crystal.

Infrared spectra were obtained at a resolution of 4.0 cm^{-1} with a Perkin-Elmer System 2000 FTIR spectrometer, equipped with a deuterated triglycine sulfate (DTGS) detector and a Ge/KBr beam splitter. The frequency scale was internally calibrated to 0.01 cm^{-1} using a He−Ne laser. Collection of meaningful infrared spectra of gels in the transmission mode is a difficult task, especially if one is interested in measuring the absorbance of medium−strong solvent peaks. This would require the use of extremely thin liquid cells (few microns) which are difficult to fill and to clean. Therefore, FTIR spectra were collected in the attenuated total reflectance mode (ATR) using a multiple reflection ATR accessory (Benchmark from SPECAC, UK) with horizontal geometry.

Two crystals were used depending on the frequency range investigated: ZnSe from 4000 to 650 cm^{-1} and KRS-5 between 650 and 400 cm^{-1}. For both crystals the angle of incidence was 45°, and the number of reflections was equal to 6.

With this sampling technique, it was always possible to maintain the analytical peaks within the range of absorbance linearity (less than 1.2 absorbance units).

For sPS/DCE gels with concentrations below ca. 0.25 g/g a piece of gel having the dimensions of the ATR crystal was prepared beforehand in a test tube. For higher concentration gels, data were obtained by solvent desorption.

Quantitative Analysis by ATR Spectroscopy. In ATR spectroscopy the relationship between absorbance, A, and concentration of the absorbing species, C, can be expressed as

$$A = \log \frac{I_0}{I} = -\log R = \alpha n d_p C \qquad (1)$$

where I_0 is the incident intensity, I is the reflected intensity, R is the reflectivity, α is the absorption coefficient, d_p is the depth of penetration of the evanescent wave within the sample, and n is the number of reflections in the optical element. Equation 1 holds for low absorptivities, i.e., for α values not exceeding 10^4 cm^{-1}.[30,31]

One major difference between eq 1 and the Beer−Lambert relationship employed in transmission measurements is that in the former case d_p depends on the wavenumber of the incident radiation according to

$$d_p = \frac{\lambda}{2\pi n_1}\left[\sin^2 \vartheta - \left(\frac{n_2}{n_1}\right)^2\right]^{-1/2} \qquad (2)$$

where λ is the wavelength of the incident radiation, n_1 and n_2

are respectively the refractive indices of the internal reflection element (IRE) and of the sample, and θ is the incident angle.[30,32]

Thus, contrary to transmission FTIR, in ATR spectroscopy any peak has a specific path length. To take into account this effect, quantitative analysis via ATR is generally performed by band ratioing methods.[30,32] The use of this approach can also eliminate errors due to irreproducible sample contact with the IRE.

For the case of an sPS gel in DCE, the following relationships can be written:

$$A_T = \alpha_T n d_{p,T} C_T \tag{3}$$

$$A_G = \alpha_G n d_{p,G} C_G \tag{4}$$

$$A_S = \alpha_S n d_{p,S} C_S \tag{5}$$

where the subscripts T and G refer to the trans and gauche conformers of DCE and the subscript S refers to the styrene monomeric units.

Recalling that

$$C_{DCE} = C_T + C_G = \frac{1}{\alpha_T n d_{p,T}}\left(A_T + \frac{\alpha_T d_{p,T}}{\alpha_G d_{p,G}} A_G\right) \tag{6}$$

one obtains

$$\frac{C_S}{C_{DCE}} = \frac{N_S}{N_{DCE}} = \frac{\alpha_T d_{p,T}}{\alpha_S d_{p,S}} \frac{A_S}{A_T + \frac{\alpha_T d_{p,T}}{\alpha_G d_{p,G}} A_G} \tag{7}$$

where N indicates the number of moles.

Figure 1 displays a plot of N_S/N_{DCE} vs $A_S/[A_t + (\alpha_T d_{p,T}/\alpha_G d_{p,G})A_G]$ constructed by several gel samples having precisely known concentration ratios. To obtain a polymer concentration at the surface of the samples close to the bulk concentration, solvent evaporation was minimized, and the pressure applied to the sample was maintained very low in order to avoid the formation of a solvent layer on the crystal surface. The value of $\alpha_T d_{p,T}/\alpha_G d_{p,G}$ has been estimated from the ATR spectrum of liquid DCE and from the knowledge of the C_T/C_G ratio characteristic of liquid DCE at 25 °C (0.35).[33] As predicted by eq 7, the plot is linear through the origin, which allows one to evaluate spectroscopically the concentration ratio in any gel sample.

The analytical peaks employed in the present investigation were the CH_2 wagging modes of the trans and gauche DCE conformers at 1232 and 1284 cm^{-1}, respectively, and the conformationally insensitive mode of sPS at 1493 cm^{-1}.

Results

X-ray Diffraction Investigations. In Figure 2, X-ray diffraction patterns of sPS/DCE gels prepared at different polymer concentrations (a−c) are compared with typical X-ray diffraction patterns of a desiccated gel (d) and of a semicrystalline clathrate sample obtained by DCE sorption into an amorphous sample (e).

For polymer concentrations below 0.05 g/g, the amount of crystallites formed in gels is too small, and diffraction patterns do not display any Bragg peak. By increasing the polymer concentration, the crystallinity of gel samples increases, and for a gel prepared at 0.15 g/g weak peaks can be observed at $2\theta \approx 18°$, 21°, 22°, and 29°. By increasing further the polymer concentration, diffraction peaks become sharper and more intense, and for a gel prepared at 0.35 g/g, the diffraction pattern (Figure 2c) displays all the Bragg peaks observed for the semicrystalline clathrate sample (Figure 2e). It is also worth noting that desiccation of the gels leads to samples which present X-ray diffraction patterns substantially identical to those of clathrate ones. For instance, a gel sample after partial desiccation to 0.71 g/g presents the X-ray diffraction pattern shown in Figure 2d very similar to that one of Figure 2e.

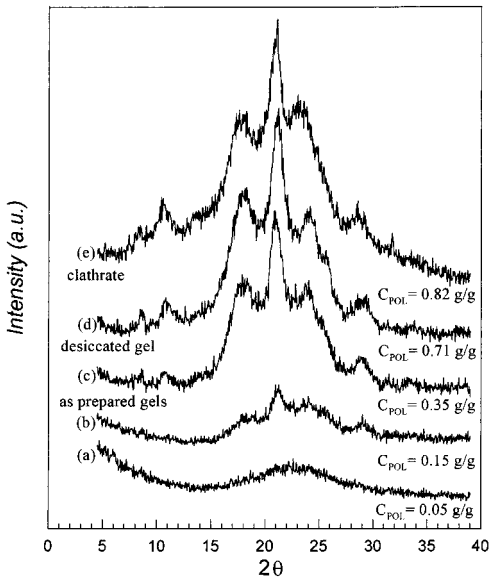

Figure 2. X-ray diffraction patterns for gels and a clathrate obtained in DCE: (a−c) as-prepared gels; (d) desiccated gel; (e) clathrate. Concentrations are expressed as polymer weight fraction.

We can also note that, in comparison to the equatorial reflections located at $2\theta = 8.2°$ (010) and $2\theta = 10.8°$ ($\bar{2}10$), the intensities of first layer peaks at $2\theta = 18°$ ((111), ($\bar{1}21$), and ($\bar{2}21$)), 21° ((321), (211), and (301)), and 24° ((121), ($\bar{4}11$), and ($\bar{4}21$)) and specially of second layer peaks at $2\theta = 29°$ ((302) and (322)) are more intense in the gels than in clathrate samples. This effect is particularly noticeable for the low-concentration gels. For instance, while the reflection at $2\theta = 29°$ is already present in the diffraction pattern of the 0.15 g/g, the equatorial reflections at $2\theta = 8.2°$ and $2\theta = 10.8°$ are barely shown.

Typical X-ray diffraction patterns of CP gels and clathrates are shown in Figure 3. As previously observed with DCE, the diffraction patterns show that the same crystalline structure is present in sPS clathrates and desiccated gels formed with CP. We can also note that for the gel sample prepared at $C_{POL} = 0.10$ g/g essentially only one diffraction peak located at $2\theta = 21°$ is present. This peak could correspond to the most intense first layer peak of the clathrate form.

These results suggest that the DCE and CP gels, at least for polymer concentrations larger than 0.10 g/g, could include clathrate phases with a large disorder (low coherent lengths) perpendicular to the chain axis while the higher persistence of the nonequatorial reflections suggests that a higher order along the chain axes would be maintained.

FTIR Investigations. a. Study of Conformation-Sensitive Polymer Bands. Infrared spectroscopy is a very sensitive tool to investigate changes in the local conformation of polymer chains, and the FTIR characterization of the different conformations and crystalline forms of sPS has been discussed by many authors.[4−6] In particular, the s(2/1)2 helical conformation exhibits characteristic absorption bands at 1355, 1277, 1169, 935, 769, 572, 549, and 502 cm^{-1}. The critical sequence length (CSL), which is defined as the lower sequence

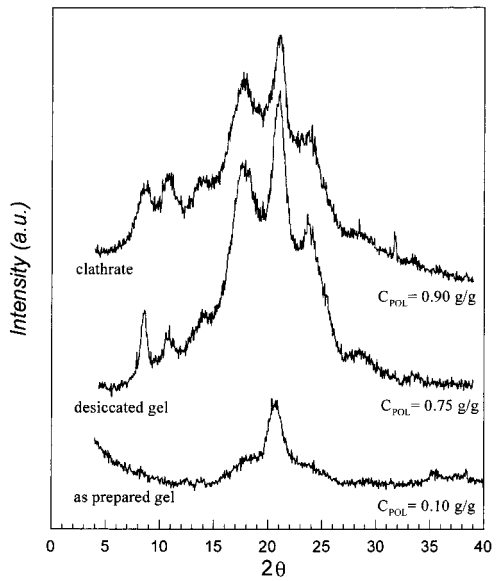

Figure 3. X-ray diffraction patterns for gels and a clathrate obtained in CP. Concentrations are expressed as polymer weight fraction.

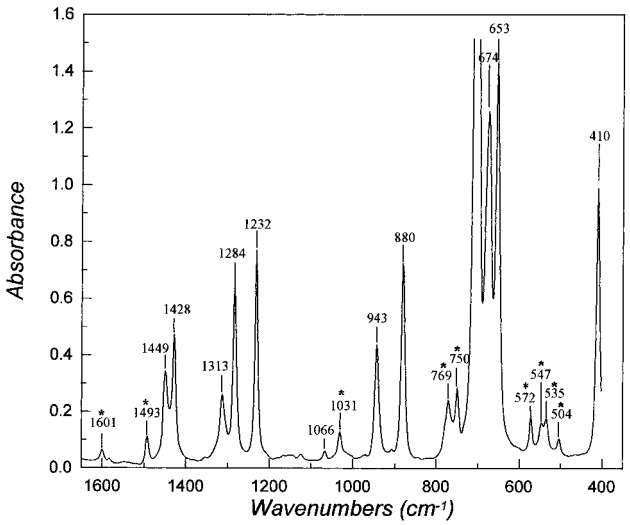

Figure 4. Infrared spectrum of a sPS/DCE gel prepared at C_{POL} = 0.05 g/g collected in the ATR mode using a KRS5 crystal. Absorption bands of sPS are indicated with asterisks.

length necessary for the appearance of the sensitive band, has been estimated for various sPS bands through the intramolecular isotope dilution technique.[34] For example, for the absorption bands centered at 1169 and 1355 cm^{-1}, the values of CSL, expressed as the number of monomeric units constituting the sequence, are respectively $m = 20-30$[35] and $m = 12-15$.[35]

Figure 4 shows the spectrum of a gel prepared in DCE at C_{POL} = 0.05 g/g collected in the ATR mode using a KRS5 crystals where polymer absorption bands are marked with asterisks. We can observe that several polymer and solvent peaks remain within the range of absorbance linearity. It is also worth noticing that absorption bands due to the s(2/1)2 helical conformation at 769, 572, 549, and 502 cm^{-1} are already clearly shown while diffraction pattern of the same sample (Figure 2a) does not display any Bragg peak.

Among the different bands sensitive to the s(2/1)2 helical conformation, we chose to consider the bands located at 1355, 1169, and 769 cm^{-1}. This choice was

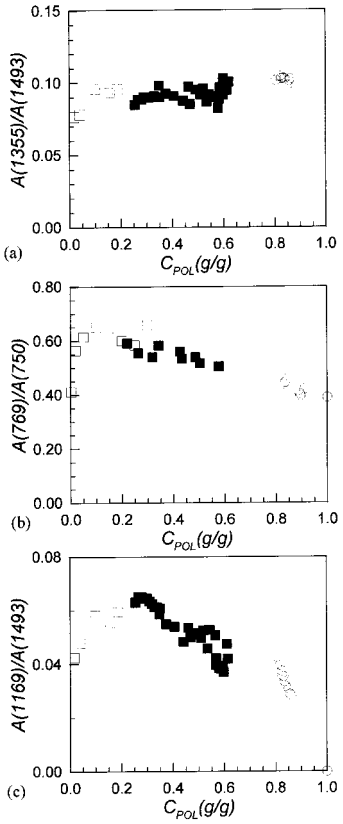

Figure 5. Variation of the reduced intensity of the 1355 cm^{-1} band (a), 769 cm^{-1} band (b), and 1169 cm^{-1} band (c) vs polymer concentration: □, as-prepared gels; ■, partially desiccated gels; ○, clathrate samples.

motivated by two reasons: (a) these bands allowed us to investigate the amount of short and long TTGG sequences as the 1355 cm^{-1} band is associated with short helical sequences while the 1169 and 769 cm^{-1} bands are associated with long helical sequences; (b) the three bands are relatively free from interfering absorption bands due to the solvent.

To minimize the effect of the difference in contact efficiency between gels and clathrates, it is necessary to use internal reference bands located not far from the sensitive bands under study. In particular, for the 769 cm^{-1} band, the internal reference band at 750 cm^{-1} was considered while for the 1355 and 1169 cm^{-1} bands, we used the reference band at 1493 cm^{-1}.

The variation of the reduced intensity of the 1355, 769, and 1169 cm^{-1} bands vs polymer concentration for gel and clathrate samples prepared with DCE is shown in parts a, b, and c of Figure 5, respectively.

In Figure 5a, we can observe, that for gel samples the intensity of the band at 1355 cm^{-1} is substantially constant within experimental uncertainty. For clathrate samples, the reduced intensity of the 1355 cm^{-1} band remains constant at a value close to that of the gel sample. These data indicate that the amount of short ($m = 12-15$) helical sequences is similar in clathrate samples and high concentration gels.

The band at 769 cm^{-1} (Figure 5b) presents a behavior that differs from that one of the 1355 cm^{-1} band. In fact, the reduced intensities display for concentrations below C_{POL} = 0.1 g/g a sharp increase with increasing polymer concentration, reaching a maximum for $C_{POL} = 0.1-0.2$ g/g. Then the reduced intensities decrease regularly with increasing polymer concentration going from gels

through desiccated gels until clathrate samples. The data relative to the 769 cm^{-1} band can be interpreted by assuming that the amount of long helical sequences is larger in gel samples than in clathrates.

As can be seen in Figure 5c, the variation of the 1169 cm^{-1} band is similar to the 769 cm^{-1} bands. For low-concentration gels, the reduced intensity of the 1169 cm^{-1} band starts to increase sharply with increasing polymer concentration before reaching a maximum at $C_{POL} = 0.25$ g/g and then, for partially desiccated gels and clathrate samples, decreases in a nearly continuous way. However, conversely to the other s(2/1)2 helical sensitive bands, the 1169 cm^{-1} band becomes negligible for the limiting emptied nanoporous δ-form ($C_{POL} = 1.0$ g/g). This observation deserves a short discussion relative to the nature of the 1169 cm^{-1} band.

As mentioned before, the IR band located at 1169 cm^{-1} has been proposed to be associated with long-ordered s(2/1)2 helical sequences.[35] However, by reducing the DCE concentration, the intensity of this band is reduced, and after complete guest removal (when the nanoporous δ-phase is obtained) this band is absent while the other s(2/1)2-sensitive bands at 769 and 1355 cm^{-1} are still present with strong intensities also after guest removal. This observation clearly indicates that the 1169 cm^{-1} band not only is a helical-sensitive band but also depends on other parameters.

For a large number of guest molecules, we have observed that all clathrate structures display a characteristic polymer peak at 1169 cm^{-1} whose intensity changes substantially with solvent type and always is reduced by reducing guest concentration, going eventually to zero after complete guest removal. It has been also shown that the intensity of the 1169 cm^{-1} band is strongly reduced when the clathrate samples are transformed into the γ-form,[36] while at the same time the intensity of the other s(2/1)2 helical-sensitive bands remains unchanged or even increases after complete formation of the γ-form.[7,37,38]

From these observations and our results, we may suggest that the peak at 1169 cm^{-1} is not only characteristic of the s(2/1)2 helical conformation but also depends on the polymer−solvent interactions occurring in the clathrate phase. Further studies on the vibrational origin of this band are in progress.

B. Study of Conformation-Sensitive Solvent Bands. As mentioned in the Introduction, information concerning the conformational equilibrium of solvent molecules can be obtained in addition to information relative to the polymer conformation.

For the evaluation of the DCE conformers, the CH_2 wagging of the trans conformer at 1232 cm^{-1} and the CH_2 wagging of the gauche conformer at 1284 cm^{-1} were used. As discussed in detail in ref 15a, the molar fraction of the trans conformer (x_T) can be evaluated by

$$x_T = \frac{1}{1 + \frac{N_G}{N_T}} = \frac{1}{1 + \frac{\alpha_T d_{p,T}}{\alpha_G d_{p,G}} \frac{A_G}{A_T}} \qquad (8)$$

where A is the absorbance, α is the absorption coefficient, d_p is the depth of penetration, and N represents the number of moles.

The ratio $\alpha_T d_{p,T}/\alpha_G d_{p,G}$ has been evaluated from the value of (x_T) in the liquid phase reported in the literature (0.35)[33] and from the absorbance ratio of the two analytical peaks in the ATR spectrum of liquid DCE.

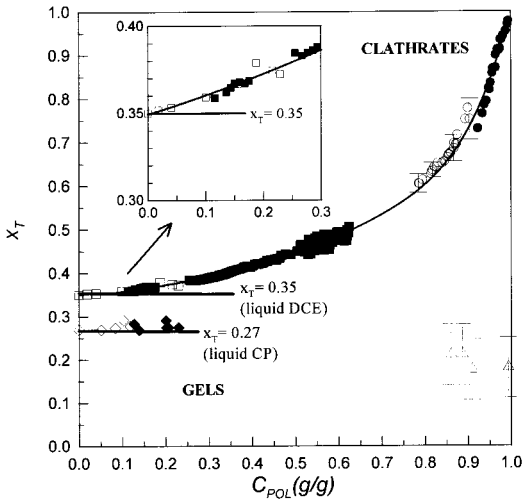

Figure 6. Fraction of trans conformer as a function of polymer concentration: □, sPS/DCE gels prepared at a given polymer concentration; ■, partially desiccated sPS/DCE gels; ○, sPS/DCE clathrates; ●, partially filled sPS/DCE clathrates obtained from a δ-form film immersed in a 0.5 wt % aqueous solution of DCE (data by Guerra et al.[16]); ◇, sPS/CP gels; ◆, partially desiccated sPS/CP gels; △, sPS/CP clathrates obtained from a δ-form film immersed in pure CP liquid (data by Guerra et al.[16]). The inset shows variations relative to diluted gels.

The fraction of DCE being in the trans conformation (x_T) as a function of polymer concentration (C_{POL}) is reported in Figure 6, for as-prepared gels as well as for partially desiccated gels and clathrate samples.

The inset of Figure 6 shows that, even for extremely diluted gels, the conformational equilibrium of DCE slightly differs from that observed in the pure liquid, i.e., $x_T = 0.35$. We can observe that the molar fraction of trans conformer increases regularly with increasing polymer concentration going from gel to desiccated gels and then to clathrates and partially emptied clathrates, reaching a value close to 1, typical of DCE in the clathrate phase.[15a,b]

The regular increase of the fraction of trans conformer observed in Figure 6, going from pure solvent to pure polymer, can be interpreted by assuming a clathrate phase as crystalline polymer-rich phase for all sPS/DCE gels. In fact, for gels with low polymer concentration only a small fraction of the solvent is included in the crystalline phase, and as a consequence, the fraction of DCE being in the trans conformation is very close to the liquid-state equilibrium, i.e., $x_T = 0.35$. When the polymer concentration increases, the amount of DCE included in the crystalline phase and hence the fraction of DCE trans conformer both increase.

For the evaluation of CP conformers, the CH_2 wagging of the trans conformer at 1337 cm^{-1} and the CH_2 wagging of the gauche conformer at 1305 cm^{-1} were used. The variation of the fraction of CP being in the trans conformation (x_T) as a function of polymer concentration (C_{POL}) is also reported in Figure 6, for as-prepared gels as well as for partially desiccated gels and clathrate samples. Data reported in Figure 6 for clathrate samples obtained with CP were previously published by Guerra et al.[16]

For gel and clathrate samples, the fraction of trans conformer changes only slightly with respect to the value of the liquid-state equilibrium, i.e., $x_T = 0.27$. Hence gels, as clathrates, do not display any conformational selectivity for CP in their crystalline phases.

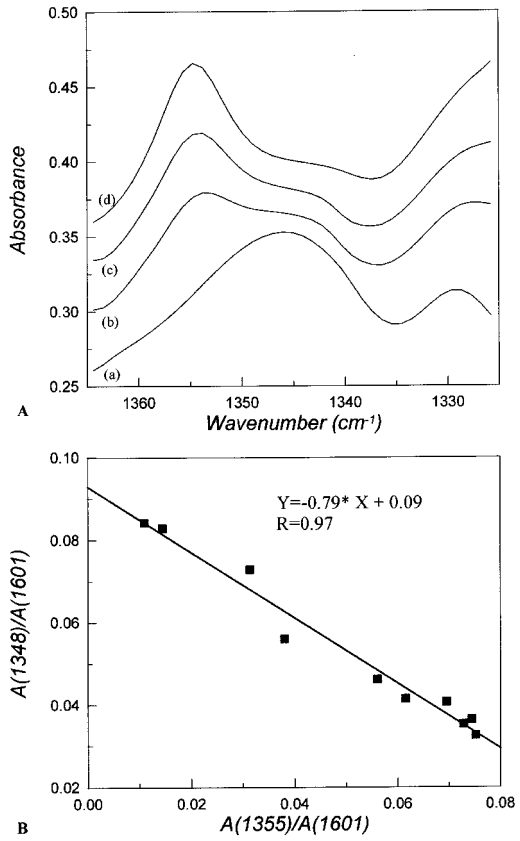

Figure 7. (A) FTIR spectral changes for amorphous sPS exposed to DCE in different conditions. (B) Variation of the reduced intensity of the 1348 cm^{-1} band corresponding to disordered polymer conformations vs the reduced intensity of the 1355 cm^{-1} band corresponding to s(2/1)2 helical sequences equal to or longer than 12−15 monomeric units for different semicrystalline clathrate samples.

Discussion

Fraction of Monomeric Units Assuming the Helical Conformation in Gel and Clathrate Samples. The fraction of styrene monomeric units accommodated in s(2/1)2 helical sequences equal to or longer than 12−15 ($x_{S,1355}$) can been estimated for both gel and semicrystalline clathrate samples in the entire range of compositions by ATR spectroscopy.

In fact, from the relationship

$$\frac{A_{1355}}{A_{1493}} = \frac{\alpha_{1355} d_{p,1355}}{\alpha_{1493} d_{p,1493}} x_{S,1355} = K x_{S,1355} \qquad (9)$$

it is possible to evaluate $x_{S,1355}$ for any sample from its ATR spectrum once the value of the constant K has been determined.

The value of the constant K has been evaluated from semicrystalline clathrate samples obtained by immersion of an amorphous film in DCE.

The value of $x_{s,1355}$ for these semicrystalline clathrate samples was determined through quantitative analysis of the IR bands at 1355 and 1348 cm^{-1} that are characteristic of ordered helical sequences and disordered conformation sequences, respectively,[39] following the procedure reported in previous works.[18,25,39] This analysis was done on transmission spectra rather than ATR spectra, due to their higher quality.

In Figure 7A the transmission FTIR spectra of a glassy sPS film (a) exposed to DCE in different conditions (b−d) are shown. The disordered conformation band at 1348 cm^{-1} decreases, while at the same time, the helical conformation band at 1355 cm^{-1} increases. For a two-component system constituted of helical and disordered sequences, Beer−Lambert's law may be expressed as

$$\frac{A_{1355}}{A_{1601}} = \frac{\epsilon_{1355}}{\epsilon_{1601}} x_{S,1355} \qquad (10)$$

$$\frac{A_{1348}}{A_{1601}} = \frac{\epsilon_{1348}}{\epsilon_{1601}} x_{S,1348} \qquad (11)$$

where ϵ represents the molar absorptivity, $x_{S,\,1355}$ is the fraction of helical styrenic units, and $x_{S,1348}$ is the fraction of conformationally disordered styrenic units. By assuming $x_{S,1355} + x_{S,1348} = 1$, we obtain

$$\frac{A_{1348}}{A_{1601}} = \frac{\epsilon_{1348}}{\epsilon_{1601}} - \frac{\epsilon_{1348}}{\epsilon_{1355}} \frac{A_{1355}}{A_{1601}} \qquad (12)$$

Figure 7B shows that a plot of A_{1348}/A_{1601} vs A_{1355}/A_{1601} for clathrate samples having different fractions of helical sequences gives a single straight line whose slope, according to eq 12, is equal to $-(\epsilon_{1348}/\epsilon_{1355})$. Rearranging eq 10 and eq 11, we have

$$\frac{1}{x_{S,1355}} = 1 + \frac{A_{1348}}{A_{1355}} \frac{\epsilon_{1355}}{\epsilon_{1348}} \qquad (13)$$

which allows to evaluate the fraction of helical sequences from the absorbance values of 1348 and 1355 cm^{-1} bands of transmission FTIR spectra and from the experimental value of $(\epsilon_{1348}/\epsilon_{1355})$.

From the above analysis it emerges that, for semicrystalline clathrate samples obtained by immersion of an amorphous film in DCE, $x_{S,1355} \approx 65\%$. As for these samples the ATR spectroscopy gives $A_{1355}/A_{1493} \approx 0.1$ (see Figure 5a), we obtain, according to eq 9, a K value of 0.154.

Then, from the experimental value of K and by using eq 9, $x_{S,1355}$ values of gels and clathrates can be evaluated in the entire range of compositions (Figure 8A).

Following the same procedure, the amount of styrene monomeric units accommodated in longer helical sequences for the 769 cm^{-1} peak ($x_{S,769}$) was estimated for the entire range of compositions, and results are shown in Figure 8B.

Figure 8A shows that, in going from clathrates to gels, the fraction of polymer included in short helical sequences remains substantially constant. However, it is worth noting that the fraction of polymer included in long helical sequences can be larger in gel samples than in clathrates (see Figure 8B). For as-prepared gels with polymer concentration larger than $C_{POL} = 0.02$ g/g, the amount of long helical sequences for the 769 cm^{-1} peak is equal to $x_{S,769} \approx 55\%$ while for clathrate samples we have $x_{S,769} \approx 37\%$. It is also worth emphasizing that the fraction of polymer included in helical sequences for semiclathrate samples ($x_{S,1355} \approx 65\%$) is consistent with a previous study where it was found that, in sPS/toluene clathrates, ca. 70% of monomer units are included in helical sequences with $m = 12-15$.[39]

Fraction of DCE Included in the Crystalline Phase of Gel and Clathrate Samples. For clathrate samples, the fraction of DCE included in the crystalline phase $x_{DCE,\,c}$ and in the amorphous phase $x_{DCE,\,am}$ can

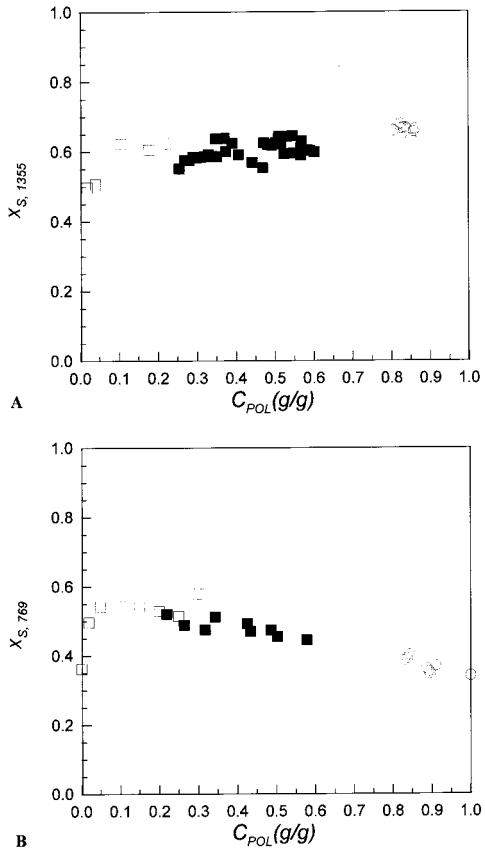

Figure 8. (A) Fraction of monomeric units included in helical sequences equal to or longer than 12−15 monomeric units ($x_{S,1355}$) as a function of the polymer weight fraction. (B) Fraction of monomeric units included in helical sequences for the 769 cm^{-1} peak ($x_{S,769}$) as a function of polymer weight fraction. □, as-prepared gels; ■, partially desiccated gels; ○, semicrystalline clathrate samples.

be estimated as in previous papers[15a,b] from the x_T values reported in Figure 6 by considering that in the amorphous phase x_T is equal to 0.51 while in the crystalline phase x_T is equal to 0.94.

For gel samples, the fraction of DCE in the crystalline phase can be also estimated from the x_T values by assuming two species of solvent molecules: bound molecules included in crystalline domains and free molecules merely entrapped in the gel network. For the former molecules, the fraction of trans conformer is assumed to be equal to the x_T value observed in the crystalline phase of semicrystalline clathrate samples, i.e., $x_T = 0.94$. For the free solvent molecules, we assumed the conformational equilibrium observed in the liquid state, i.e., $x_T = 0.35$. Of course, this assumption can be considered valid for low polymer concentration gels while it is only a rough approximation for desiccated gels corresponding to polymer concentration larger than $C_{POL} = 0.35$ g/g.

The variation of $x_{DCE,c}$ and $x_{DCE,free}$ for gels and of $x_{DCE,c}$ and $x_{DCE,am}$ for clathrates as a function of the molar fraction of styrene units ($x_S = N_S/(N_S + N_{DCE})$) is shown in Figure 9.

For gels, the fraction of DCE included in the crystalline phase gradually increases with increasing polymer concentration, while at the same time the fraction of free solvent in the gel network decreases. For low polymer concentrations, the amount of crystallites formed in the gel is very small, and $x_{DCE,c}$ is almost nought while about 25% of the DCE would be included

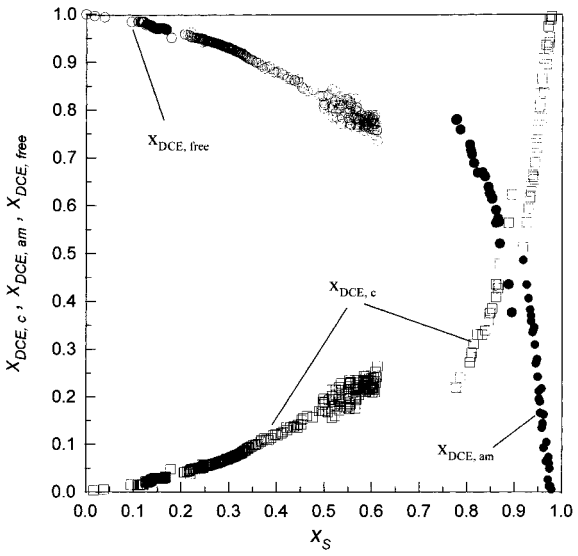

Figure 9. Fraction of DCE included in the crystalline phase ($x_{DCE,c}$, □) or in the amorphous phase ($x_{DCE,am}$, ●) or merely entrapped in the gel network ($x_{DCE,free}$, ○) as a function of the molar fraction of styrene units (x_S).

in the crystalline phase at $x_S = 0.60$ mol/mol. For semicrystalline clathrate samples, a steeper increase of $x_{DCE,c}$ with increasing polymer concentration is observed, and for $x_S > 0.97$ almost all DCE molecules are included as a guest in the clathrate phase.

Stoichiometry of the Crystalline Phase of sPS/DCE Gels and Clathrates. The ratio $N_{S,h}/(N_{S,h} + N_{DCE,c})$, where $N_{S,h}$ is the number of styrene monomeric units in the helical conformation and $N_{DCE,c}$ the number of solvent molecules included in the crystalline phase, can be considered as a stoichiometric ratio of the clathrate phase in the assumption that all the helical sequences are included into the crystalline phase. This ratio, calculated from $x_{S,1355}$ and $x_{DCE,c}$ values reported in Figure 8A and Figure 9, respectively, is reported vs the molar fraction of styrene units (x_S) for gels and clathrates in Figure 10 (filled symbols).

For semicrystalline clathrate samples, an additional evaluation of the stoichiometric ratio of the clathrate phase can be obtained by the ratio $N_{S,R-X}/(N_{S,R-X} + N_{DCE,c})$, where $N_{S,R-X}$ is the number of styrene units in the crystalline phase, as evaluated by wide-angle X-ray diffraction crystallinity. The measured crystallinity estimated from the diffraction pattern of a clathrate sample obtained by immersion of an amorphous film in pure DCE (Figure 2e) was assumed to remain nearly constant for all the considered semicrystalline clathrate samples (ca. 33%). These evaluations have also been reported in Figure 10 as empty symbols.

For clathrates, besides data relative to samples obtained by immersion of amorphous films in pure liquid DCE or δ-form films in DCE aqueous solutions (circles), also data relative to samples obtained by desiccation for different times at 50 °C of the clathrate samples presenting $x_S \approx 0.8$ (square symbols) are reported.

The stoichiometry of the crystalline phase which has been established for sPS clathrates with DCE, corresponding to four monomeric units per guest molecule,[12] is also indicated as a dashed line in Figure 10.

We can observe that for gels the ratio $N_{S,h}/(N_{S,h} + N_{DCE,c})$ is substantially constant within experimental uncertainty (0.78 ± 0.02), i.e., $N_{S,h}/N_{DCE,c} = 3.6 \pm 0.3$.

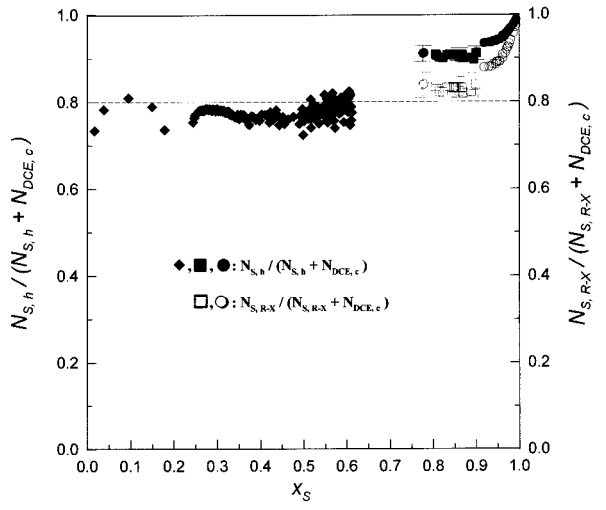

Figure 10. Molar fraction of styrenic units included in the crystalline phase as a function of the molar fraction of styrene units determined as: (1) $N_{S,h}/(N_{S,h} + N_{DCE,c})$, where $N_{S,h}$ is the number of styrenic units in the helical conformation and $N_{DCE,c}$ is the number of guest molecules included in the crystalline phase, for gels samples (◆), freshly prepared semicrystalline clathrate samples (●), and partially desiccated clathrates (■); (2) $N_{S,R-X}/(N_{S,R-X} + N_{DCE,c})$, where $N_{S,R-X}$ is the number of styrene units in the crystalline phase as evaluated by X-ray diffraction measurements and $N_{DCE,c}$ is the number of guest molecules included in the crystalline phase, for freshly prepared semicrystalline clathrate samples (○) and partially desiccated clathrates (□).

Hence, two independent evaluations by FTIR measurements of fraction of sPS helices and of DCE in the clathrate phase, for several gel samples, resulted in a stoichiometric ratio for the polymer-rich phase substantially coincident with the stoichiometry of the sPS/DCE clathrate phase, as determined by structure factor calculations relative to X-ray diffraction patterns of fibers.[12]

For semicrystalline clathrate samples obtained with amorphous films immersed in pure liquid DCE and then desiccated at 50 °C, for different times, the evaluated stoichiometric ratios remain also constant. This constancy of the stoichiometric ratios evaluated for the crystalline phase is consistent with the well-characterized desorption phenomena for sPS clathrate samples, which prevailingly involves DCE molecules from the amorphous phase.[15b] It is worth noting that the ratio $N_{S,R-X}/(N_{S,R-X} + N_{DCE,c})$ remains close to the stoichiometric ratio of the clathrate crystalline structure (0.83 ± 0.01) while the ratio $N_{S,h}/(N_{S,h} + N_{DCE,c})$ is definitely larger (0.91 ± 0.02).

For freshly prepared clathrate samples (circles), by increasing x_S above 0.8, the stoichiometric ratios increase with decreasing the solvent concentration and the increase becomes steep for $x_S > 0.95$. This increase is, of course, due to the progressive removal of DCE from the clathrate phase, which eventually becomes the nanoporous δ-form. Also, for these samples the stoichiometric ratio based on the helical chains is substantially larger than those relative to the crystalline phase, as evaluated by X-ray diffraction measurements.

In general, for semicrystalline polymeric samples, it is well-known that the fraction of polymer assuming the conformation typical of the crystalline phase, as determined by infrared measurements, can be substantially larger than the fraction of polymer included in the crystalline phase, as determined by X-ray diffraction measurements. This difference is generally rationalized in terms of some mesomorphic ordering of the polymer chains assuming the regular conformations typical of the crystalline phases. It is worth noticing that the formation of a helical mesomorphic ordering has been already observed for sPS samples, by different techniques.[37,40]

In particular, for clathrate samples obtained by DCE sorption into an amorphous sample (square symbols in Figure 10), we evaluated the polymer fraction assuming the helical s(2/1)2 conformation close to 65% (Figure 8a) while the polymer fraction in the crystalline phase would be only 33% (evaluated by the X-ray diffraction pattern of Figure 2e). A corresponding rough evaluation of the polymer fraction in the mesophase (32%) is qualitatively consistent with that one obtained by methylene chloride diffusion measurements into amorphous sPS samples (25%).[40c]

Conclusions

Comparative FTIR and X-ray diffraction characterizations of gel and clathrate samples have allowed to clarify the nature of the polymer-rich phase of sPS/DCE and sPS/CP gels.

In fact, the following experimental results indicate that the polymer-rich phase forming the cross-links domains of these gels is a crystalline clathrate phase: (i) the similarity of FTIR spectra of sPS in gel and in clathrate samples; (ii) the presence of X-ray diffraction peaks typical of the sPS/DCE and sPS/CP clathrate structures, at least for gels with polymer concentration larger than 0.1 g/g; (iii) the occurrence of the same kind of conformational selectivity for DCE (in favor of the trans conformer) and the absence of conformational selectivity for CP for both gel and clathrate samples; and (iv) the FTIR evaluation of the stoichiometry of the crystalline phase, which is nearly constant (3.6 ± 0.3) for the entire gel composition range and is very close to the ratio (4) typical of the clathrate crystalline structure.

As for the morphology of the crystalline phase in gels, the faster disappearance of the equatorial reflections with respect to the nonequatorial ones, going from X-ray diffraction patterns of clathrates to those of gels, suggests the occurrence of lower coherent lengths perpendicular to the chain axes while a higher order along the chain axes would be maintained. This conclusion is consistent with the increase of polymer fraction included in long helical sequences ($m = 20-30$) which is observed going from clathrates to gels.

Acknowledgment. C.D. was supported by a grant cofinanced by EEC (European Social Fund). We thank Dr. V. Venditto from Dipartimento di Chimica (University of Salerno) for useful discussions, Ennio Comunale from Dipartimento di Ingegneria Chimica ed Alimentare (University of Salerno) for the GPC measurements, A. Mandanis for assistance in the experimental work, and Dow Chemicals for the gift of Questra 101. The financial support of MURST of Italy (Grant Cluster 26) is also acknowledged.

References and Notes

(1) Ishihara, N.; Seimiya, T.; Kuramoto, M.; Uoi, M. *Macromolecules* **1986**, *19*, 2465.
(2) Immirzi, A.; De Candia, F.; Iannelli, P.; Vittoria, V.; Zambelli, A. *Makromol. Chem. Rapid Commun.* **1988**, *9*, 761.
(3) Vittoria, V.; De Candia, F.; Iannelli, P.; Immirzi, A. *Makromol. Chem. Rapid Commun.* **1988**, *9*, 765.

(4) Kobayashi, M.; Nakaoki, T.; Ishihara, N. *Macromolecules* **1989**, *22*, 4377.
(5) Kobayashi, M.; Nakaoki, T.; Ishihara, N. *Macromolecules* **1990**, *23*, 78.
(6) Guerra, G.; Vitagliano, V. M.; De Rosa, C.; Petraccone, V.; Corradini, P. *Macromolecules* **1990**, *23*, 1539.
(7) Guerra, G.; Musto, P.; Karaz, F. E.; MacKnight, W. J. *Makromol. Chem.* **1990**, *191*, 2111.
(8) De Rosa, C.; Guerra, G.; Petraccone, V.; Corradini, P. *Polym. J.* **1991**, *23*, 1435.
(9) Chatani, Y.; Shimane, Y.; Inagaki, T.; Ijitsu, T.; Yukinari, T.; Shikuma, H. *Polymer* **1993**, *34*, 1620.
(10) Chatani, Y.; Inagaki, T.; Shimane, Y.; Shikuma, H. *Polymer* **1993**, *34*, 4841.
(11) De Rosa, C.; Guerra, G.; Petraccone, V.; Pirozzi, B. *Macromolecules* **1997**, *30*, 4147.
(12) De Rosa, C.; Rizzo, P.; Ruiz de Ballesteros, O.; Petraccone, V.; Guerra, G. *Polymer* **1999**, *40*, 2103.
(13) Guerra, G.; Manfredi, C.; Rapacciuolo, M.; Corradini, P.; Mensitieri, G.; Nobile, M. A. Ital. Pat., 1994 (CNR). (b) Reverchon, E.; Guerra, G.; Venditto, V. *J. Appl. Polym. Sci.* **1999**, *74*, 2077.
(14) Manfredi, C.; Del Nobile, M. A.; Mensitieri, G.; Guerra, G.; Rapacciuolo, M. *J. Polym. Sci., Polym. Phys. Ed.* **1997**, *35*, 133.
(15) Guerra, G.; Manfredi, C.; Musto, P.; Tavone, S. *Macromolecules* **1998**, *31*, 1329. (b) Musto, P.; Manzari, M.; Guerra, G. *Macromolecules* **1999**, *32*, 2770. (c) Musto, P.; Manzari, M.; Guerra, G. *Macromolecules* **2000**, *33*, 143.
(16) Guerra, G.; Milano, G.; Venditto, V.; Musto, P.; De Rosa, C.; Cavallo, L. *Chem. Mater.* **2000**, *12*, 363.
(17) Kobayashi, M.; Kosaza, T. *Appl. Spectrosc.* **1993**, *9*, 1417.
(18) Kobayashi, M.; Yoshioka, T.; Imai, M.; Itoh, Y. *Macromolecules* **1995**, *28*, 7376.
(19) Daniel, C.; Dammer, C.; Guenet, J. M. *Polymer* **1994**, *19*, 4243.
(20) Daniel, C.; Deluca, M. D.; Guenet, J. M.; Brulet, A.; Menelle, A. *Polymer* **1996**, *7*, 1273.
(21) Daniel, C.; Menelle, A.; Brulet, A.; Guenet, J. M. *Polymer* **1997**, *16*, 4193.
(22) Prasad, A.; Mandelkern, L. *Macromolecules* **1990**, *23*, 5041.
(23) Deberdt, F.; Berghmans, H. *Polymer* **1993**, *34*, 2192.
(24) Deberdt, F.; Berghmans, H. *Polymer* **1994**, *35*, 1694.
(25) Kobayashi, M. *Macromol. Symp.* **1997**, *114*, 1.
(26) Li, Y.; Xue, G. *Macromol. Rapid Commun.* **1998**, *19*, 549.
(27) For sPS/iodine clathrate the stoichiometry is 2/1 monomeric units/solvent molecule.[10]
(28) Roels, T.; Deberdt, F.; Berghmans, H. *Macromolecules* **1994**, *27*, 6216.
(29) Rastogi, S.; Goossens, J. G. P.; Lemstra, P. J. *Macromolecules* **1998**, *31*, 2983.
(30) Harrick, N. J. *Internal Reflection Spectroscopy*; Harrick Scientific Corp.: New York, 1967.
(31) Flournoy, P. A. *Spectrochim. Acta* **1966**, *22*, 5.
(32) Mirabella, F. M. *Appl. Spectrosc. Rev.* **1985**, *21*, 45.
(33) Tanabe, K. *Spectrochim. Acta* **1972**, *28A*, 407.
(34) Kobayashi, M.; Akita, K.; Tadokoro, H. *Makromol. Chem.* **1968**, *118*, 324.
(35) Tashiro, K.; Ueno, Y.; Yoshioka, A.; Kaneko, F.; Kobayashi, M. *Macromolecules* **2001**, *34*, 310.
(36) De Candia, F.; Guadagno, L.; Vittoria, V. *J. Macromol. Sci., Phys.* **1995**, *B34*, 95.
(37) Manfredi, C.; De Rosa, C.; Guerra, G.; Rapacciuolo, M.; Auriemma, F.; Corradini, P. *Macromol. Chem. Phys.* **1995**, *196*, 2795.
(38) Nakaoki, T.; Kobayashi, M. *J. Mol. Struct.* **1991**, *242*, 315.
(39) Tashiro, K.; Ueno, Y.; Yoshioka, A.; Kaneko, F.; Kobayashi, M. *Macromol. Symp.* **1999**, *141*, 33.
(40) Vittoria, V.; Ruvolo Filho, A.; De Candia, F. *Polym. Bull. (Berlin)* **1991**, *26*, 445. (b) De Candia, F.; Carotenuto, M.; Guadagno, L.; Vittoria, V. *Macromolecules* **1992**, *25*, 6361. (c) De Candia, F.; Guadagno, L.; Vittoria, V. *J. Macromol. Sci., Phys.* **1994**, *B33*, 347.

MA011531Q